Site-Directed Mutagenesis of the CP 47 Protein of Photosystem II: Alteration of Conserved Charged Residues in the Domain ^{364}E−^{444}R†

Cindy Putnam-Evans,‡ Robert Burnap,§ Jituo Wu,|| John Whitmarsh,⊥ and Terry M. Bricker*,▽

Department of Biology, East Carolina University, Greenville, North Carolina 27858, Department of Microbiology and Molecular Genetics, Oklahoma State University, Stillwater, Oklahoma 74078, Department of Plant Biology, Louisiana State University, Baton Rouge, Louisiana 70803, Photosynthesis Research Unit, USDA/ARS, Department of Plant Biology, University of Illinois, Urbana, Illinois 61201, and Department of Microbiology, Louisiana State University, Baton Rouge, Louisiana 70803

Received November 8, 1995; Revised Manuscript Received February 5, 1996⊗

ABSTRACT: The intrinsic chlorophyll-protein CP 47 is a component of photosystem II in higher plants, green algae and cyanobacteria. We had shown previously by biochemical methods that the domain ^{364}E−^{440}D of CP 47 interacts with the 33 kDa extrinsic protein of photosystem II [Odom, W. R., & Bricker, T. M. (1992) *Biochemistry 31*, 5616−5620]. In this study, using oligonucleotide-directed mutagenesis in the cyanobacterium *Synechocystis* 6803, mutations at 17 conserved charged residues were introduced into the domain ^{364}E−^{444}R of the CP 47 protein. Only mutations introduced at positions ^{384}R and ^{385}R led to a modified PS II phenotype. We previously described a mutation at (RR384385GG) which resulted in a mutant with a defective oxygen-evolving complex [Putnam-Evans, C., & Bricker, T. M. (1992) *Biochemistry 31*, 11482−11488]. An additional set of mutations, ^{384}R to ^{384}G, ^{385}R to ^{385}G, and ^{384,385}RR to ^{384,385}EE has now been introduced at this site yielding the mutants R384G, R385G, and RR384385EE, respectively. Steady state oxygen evolution measurements and quantum yield measurements demonstrated that these mutants exhibited significant alterations in their ability to evolve oxygen. Total fluorescence yield measurements indicated that all of these mutants contained about 85%−90% of the PS II reaction centers found in the control strain. This decrease was insufficient to explain the oxygen evolution results. Analysis of oxygen flash yield parameters indicated that there was little change in the S-state parameters α, β, γ, or δ. Measurement of the S_2 lifetime, however, demonstrated that the S_2 lifetime of the mutants was 2−3 times longer than that of the control. Additionally, examination of the risetime of the oxygen signal indicated that there was a significant retardation (6−7-fold) in the rate of oxygen release, suggesting a retarded S_3-[S_4]-S_0 transition. These data reinforce our hypothesis that the positive charge density at positions ^{384}R and ^{385}R in the large extrinsic loop of CP 47 is necessary for its function in water oxidation. We speculate that this positive charge density may be an important factor in establishing the proper interaction between CP 47 and the 33 kDa extrinsic protein.

Photosystem II (PS II) is a multisubunit thylakoid membrane protein complex which catalyzes the light-driven oxidation of water to molecular oxygen and the reduction of plastoquinone to plastoquinol. Seven intrinsic PS II polypeptides appear to form the minimum complex capable of water oxidation (Burnap & Sherman, 1991; Bricker, 1992). These proteins have apparent molecular masses of 49 (CP 47), 45 (CP 43), 34 (D1), 32 (D2), 9 and 4.5 (α and β subunits of cytochrome b_{559}), and 4 kDa (*psb*I gene product) (Burnap & Sherman, 1991; Bricker, 1992; Debus, 1992). Additionally, in *Synechocystis*, an extrinsic 33 kDa protein is required for optimal rates of oxygen evolution at physiological salt concentrations (Burnap & Sherman, 1991) wheras in higher plants and algae proteins of 33, 24, and 17 kDa are required. The inorganic cofactors manganese, calcium, and chloride are also required for oxygen evolution activity. The binding sites for these cofactors within PS II are unknown (Debus, 1992).

The chlorophyll-protein CP 47, a component of the interior antenna for PS II, is an integral membrane protein which is predicted to contain six membrane-spanning α helical domains (Vermaas et al., 1987; Bricker, 1990). In addition to its role in light-harvesting, several lines of evidence indicate that the large extrinsic loop E of this protein, ^{257}W−^{450}W (Bricker et al., 1990), structurally interacts with the oxygen-evolving complex of PS II. Experiments utilizing monoclonal antibodies have demonstrated that the removal of the chloride-insensitive manganese from PS II membranes leads to a conformational change which exposes a domain of loop E (^{360}P−^{391}S) to a specific monoclonal antibody probe (Bricker & Frankel, 1987; Frankel & Bricker, 1990). In the absence of the 33 kDa extrinsic protein, two domains in loop E are labeled with the amino group-specific labeling reagent NHS-biotin (^{304}K−^{321}K and ^{389}K−^{419}K) (Frankel & Bricker, 1992). Protein cross-linking experiments using the zero-

† This work was supported by USDA-NRICGP Grants 91-37036-6350 to T.M.B., 92-37306-7820 to R.B., and 94-37306-0412 to J.W.

* Corresponding author: Phone: (504) 388-2601. E-Mail: BTBRIC@LSUVM. SNCC. LSU. EDU.

‡ East Carolina University.

§ Oklahoma State University.

|| Department of Plant Biology, Louisiana State University.

⊥ University of Illinois.

▽ Department of Microbiology, Louisiana University.

⊗ Abstract published in *Advance ACS Abstracts,* March 15, 1996.

[1] Abbreviations: DCBQ, 2,6-dichloro-*p*-benzoquinone; DCMU, 3-(3,4-dichlorophenyl)-1,1-dimethylurea; DPC, diphenylcarbazide; HEPES, *N*-(2-hydroxyethyl)-piperazine-*N*′-(2-ethanesulfonic acid); NHS-biotin, *N*-hydroxysuccinimidobiotin; PS II, photosystem II; TES, *N*-[tris-(hydroxymethyl)methyl]-2-aminoethanesulfonic acid.

0006-2960/96/0435-4046$12.00/0

length cross-linking reagent EDC have documented the formation of cross-linked products between the extrinsic loop E of CP 47 and the 33 kDa extrinsic protein (^{364}E−^{440}D of CP 47) (Bricker et al., 1988; Enami et al., 1991; Odom & Bricker, 1992). Furthermore, the loss of oxygen evolution following trypsin digestion of PS II membranes depleted of the extrinsic 33 kDa protein is correlated with the cleavage of CP 47 at ^{389}K (Hayashi et al., 1993) in spinach.

The CP 47 protein is encoded by the *psb*B gene. Insertional mutagenesis (Vermaas et al., 1987) or deletion (Eaton-Rye & Vermaas, 1991) of the *psb*B gene in the cyanobacterium *Synechocystis* 6803 leads to a PS II-minus phenotype, and it has been hypothesized that CP 47 is required for PS II assembly (Vermaas et al., 1988). A number of short deletion mutations have been produced in the large extrinsic loop (Eaton-Rye & Vermaas, 1991; Haag et al., 1993). While some of these short deletions have no apparent effect on PS II function, others have mild to severe deleterious consequences. Two particularly interesting deletion mutants, Δ(A373−D380) and Δ(R384−V392), have phenotypes consistent with a disruption of the interaction between CP 47 and the 33 kDa extrinsic protein of PS II (Eaton-Rye & Vermaas, 1991; Haag et al., 1993; Gleiter et al., 1994, 1995). However, since deletions can produce large perturbations in protein structure, the biochemical interpretation of the observed phenotypes of such mutants is difficult.

In order to examine the role of CP 47 in oxygen evolution we have been systematically modifying all of the conserved charged residues in the lumenally exposed loops of CP 47. We previously demonstrated that alteration of an arginyl pair at positions 384 and 385 to a glycyl pair produced a strain of *Synechocystis* exhibiting enhanced rates of photoinactivation, reduced numbers of fully functional PS II centers, and oxygen evolution at 50% of control rates (Putnam-Evans & Bricker, 1992). Additionally, this mutant showed an enhanced ability of DPC to act as an electron donor to PS II, indicating damage to the manganese cluster of the oxygen-evolving complex in thylakoid membranes. These results were consistent with the arginyl pair being required for stability of the oxygen-evolving complex.

In this communication we have used site-directed mutagenesis to modify all of the conserved charged residues in the domain ^{364}E to ^{440}D which we had previously shown to interact with the 33 kDa extrinsic protein (Odom & Bricker, 1992). Only mutations introduced at the arginyl residues 384 and 385 exhibited altered PS II characteristics. The phenotypes of these mutants are consistent with an alteration in the interaction between CP 47 and the extrinsic 33 kDa protein of PS II.

MATERIALS AND METHODS

Control and mutant strains of *Synechocystis* sp. PCC 6803 were grown in liquid BG-11 media (Rippka et al., 1979) supplemented with glucose at 28−30 °C at 20 μmol of photons·m^{-2}·s^{-1}. On plates, cultures were maintained on BG-11 media supplemented with 1.5% agar, 0.3% sodium thiosulfate, 10 mM TES/KOH, pH 8.2, 5 mM glucose, and 10 μM DCMU. Antibiotics were added to the media at a final concentration of 10 μg/mL.

Restriction digests, cloning, growth, and transformation of bacterial strains, and isolation of DNA fragments were performed according to standard procedures (Maniatis et al., 1992). Plasmid isolations were performed using disposable anion-exchange columns from Qiagen, Inc. The method of Kunkel et al. (1995) was employed for the oligonucleotide-mediated mutagenesis. Plasmid constructs, *Synechocystis* transformation procedures, and descriptions of the *psb*B partial deletion strain (DEL-1) and control strain K3 have been described elsewhere (Putnam-Evans & Bricker, 1992).

To demonstrate that the intended mutations were present, genomic DNA was isolated from putative mutants from cell lysates according to the procedure of Williams (1988) with the exception that the cesium chloride steps were omitted. Oligonucleotides flanking the *Kpn*I/*Kpn*I fragment of the *psb*B gene were used to amplify this region from the genomic DNA of each mutant using the polymerase chain reaction. The thermal cycling routine consisted of the following steps performed on 100 μL reaction mixtures: 1 min denaturation at 94 °C, 1 min annealing at 54 °C, and 1 min elongation at 72 °C for a total of 30 cycles. PCR products were directly cloned into the pGEM-T vector (Promega). Plasmids containing inserts were sequenced using the PRISM Ready Reaction Dyedeoxy Terminator Cycle Sequencing Kit (Applied Biosystems, Inc.) The sequencing reactions were analyzed on an automated DNA sequencer (model 373A, Applied Biosystems).

PS II activity was measured by oxygen polarography using a Hansatech oxygen electrode. Cells were assayed in BG-11 media with 1 mM DCBQ added as an electron acceptor. Oxygen evolution was measured at a light intensity of 3000 μmol of photons·m^{-2}·s^{-1} of copper sulfate filtered white light at 25 °C. For the quantum yield experiments, the light intensity was varied between 25 and 150 μmol of photons·m^{-2}·s^{-1}. Light intensity was measured with a spectroradiometer equipped with a quantum probe (Li-Cor, Inc.) For the photoinactivation experiments, cells were incubated in BG-11 media at a chlorophyll concentration of 10 μg/mL at 4000 μmol of photons·m^{-2}·s^{-1} at 25 °C. At various times, aliquots were removed, 1.0 mM DCBQ was added, and the samples were assayed for oxygen-evolving activity as described above. The chlorophyll concentration in all oxygen evolution assays was 10 μg/mL.

Variable fluorescence yield measurements were performed on a Walz PAM 101 fluorimeter as previousely described (Nixon & Diner, 1992; Chu et al., 1994). Samples (33 μg of Chl/mL) were incubated in the dark for 5 min in the presence of 1 mM potassium ferricyanide and 330 μM DCBQ. DCMU was added to a concentration of 40 μM followed 1 min later by the addition of hydroxylamine hydrochloride (pH 6.5) to a concentration of 20 mM. After 20 s the weak monitoring flashes were turned on followed 5 s later by continuous actinic illumination (1000 μmol of photons·m^{-2}·s^{-1}).

Flash oxygen yields were measured on a bare platinum electrode that permits centrifugal deposition of samples on the electrode similar to the design of Dr. Bruce Diner (personal communication). The polarization circuit and amplification circuitry (AC coupling) were constructed using a published design (Meunier & Popovic, 1988). With this design, ampermeric signals were filtered through selectable high-pass (1−10 Hz) and low pass (150−1500 Hz) filters. The high-pass filter was set to 10 Hz for these experiments, effectively subtracting slow transients due to a background of oxygen consumption at the platinum upon polarization. Polarization of the electrode (0.73 V) was initiated 15 s

Table 1: Mutagenic Oligonucleotides Used To Construct Site-Directed Alterations in the Large Extrinsic Loop E of CP 47[a]

strain	primer Sequence
RR357358GG	5′-CGG GAA CTG GAG GTA GGG GGT ATG CCT AAC TTC TTT GA-3′
E364Q	5′-CGT ATG CCT AAC TTC TTT CAG ACT TTC CCC GTC ATC AT-3′
D372N	5′-CCC GTC ATC ATG ACC AAC GCG GAT GGT GTA GTC-3′
R378G	5′-T GCG GAT GGT GTA GTC GGC GCG GAT ATT CCC TTC C-3′
D380N	5′-AT GGT GTA GTC CGG GCG AAC ATT CCC TTC CGT CGT TCC-3′
R384G	5′-CGG GCG GAT ATT CCC TTC GGT CGT TCC GAG TCT AAA TTC-3′
R385G	5′-GCG GAT ATT CCC TTC CGT GGT TCC GAG TCT AAA TTC AGT-3′
RR384385GG	5′-GG GCG GAT ATT CCC TTC GGT GGT TCC GAG TCT AAA TTC AGT GT-3′
RR384385EE	5′-TC CGG GCG GAT ATT CCC TTC GAA GAG TCC GAG TCT AAA TTC AGT GTG G-3′
E387Q	5′-ATT CCC TTC CGT CGT TCC CAG TCT AAA TTC AGT GTG GAA-3′
KK418419GG	5′-GC AAT CCC AGT GAT GTG GGG GGG TTT GCC CGG AAA GCT CA-3′
RK422423GG	5′-GAT GTG AAG AAG TTT GCC GGG GGA GCT CAG TTG GGT GAA GG-3′
E428Q	5′-CGG AAA GCT CAG TTG GGT CAA GGC TTC GAC TTC GAT AC-3′
D431N	5′-CAG TTG GGT GAA GGC TTC AAC TTC GAT ACG GAA ACC TT-3′
D440N	5′-CG GAA ACC TTC AAC TCT AAC GGT GTA TTC CGC ACC A-3′
R444G	5′-AAC TCT GAT GGT GTA TTC GGG ACC AGT CCC CGG GG-3′

[a] Codons which contain the site-directed mutations are underlined.

before the initiation of data acquisition, and the flash sequence was initiated 333 ms thereafter. The amplified electrode signal was digitized by an analog to digital/digital to analog board (AT-MIO-16F, National Instruments, Austin, TX), which also controlled the timing of the polarization of the electrode, data acquisition, and firing of the actinic xenon flashes. Dark-incubated samples containing 6 μg of Chl in 10 mM HEPES-NaOH, pH 7.1, 30 mM NaCl, were centrifuged in a removable electrode unit at 5000*g* for 5 min at 25 °C in a Sorvall HB-4A swinging bucket rotor. Estimation of the S-state transition probabilities were obtained upon analysis of the oscillatory pattern of oxygen yields during the flash sequence according to the method of Meunier (1993). For this, the oxygen signals were recorded with a low-pass filter at the 150 Hz setting to minimize the contribution of the electrical noise. Estimation of the lifetime of the S2 state of the water oxidation complex was performed according to the method of Forbush et al. (1971). Measurements of the apparent oxygen release kinetics were performed with the low-pass filter at the 1500 Hz setting to maximize the response of the electrode. Under these conditions the response time of the electrode was approximately 1 ms as estimated from the photoelectric flash artifact.

RESULTS AND DISCUSSION

Table 1 summarizes the mutagenic oligonucleotides which were employed to introduce site-specific changes in the extrinsic loop of CP 47. Following construction of these mutations which were closely linked to a kanamycin resistance gene in the plasmid pTZ18K3 (Putnam-Evans & Bricker, 1992) and sequencing to verify each mutation, the resulting plasmids were used to transform the partial deletion strain DEL-1 (Putnam-Evans & Bricker, 1992). Transformants were screened for the loss of spectinomycin resistance and the acquisition of kanamycin resistance. After several rounds of streaking, mutant colonies were isolated, their genomic DNA extracted, and the 1400 base pair *Kpn*I/*Kpn*I fragment containing the introduced mutation was amplified using the polymerase chain reaction. This fragment was cloned into the pGEM-T vector, and the resulting transformants were pooled and sequenced. The DNA sequence for each mutant demonstrated that each contained the intended mutations. No additional spurious mutations were observed in the amplified *Kpn*I/*Kpn*I fragments from any of the mutants examined (data not shown).

Figure 1 shows the results obtained when these mutants and the control strain K3 were analyzed for steady-state oxygen evolution activity. The K3 control strain of *Synechocystis* lacks any site-directed alterations but is otherwise identical to the mutant strains in that it contains the kanamycin resistance cassette in the 3′-flanking region of the *psb*B gene (Putnam-Evans & Bricker, 1992). We introduced site-directed alterations at nearly all of the conserved charged residues in the domain ^{364}E to ^{440}D, a region identified previously to interact with the 33 kDa extrinsic protein (Odom & Bricker, 1992). No mutation was introduced at the conserved glutamyl residue ^{393}E. It had earlier been shown that the deletion strain Δ(V392−Q394) was essentially normal with respect to oxygen evolution capacity (Figure 1) (Haag et al., 1993). As shown in Figure 1, only modifications at positions ^{384}R and ^{385}R exhibited a decreased rate in oxygen evolution. As we have reported previously, RR384385GG exhibits a water to DCBQ oxygen evolution rate that is 51% of the rate of the control strain K3 (Putnam-Evans & Bricker, 1992). The newly constructed mutants R384G and R385G exhibited oxygen evolution rates that were 64% and 78% of the control rate, respectively. These data demonstrate that the elimination of a positively charged residue at position ^{384}R or ^{385}R produces a strain defective in oxygen evolution activity. It is noteworthy that the calculated cumulative effect of these two mutations is a 50% decrease in oxygen evolution, which is the same as the decrease in rate observed for the double-mutant RR384385GG (Putnam-Evans & Bricker, 1992). It appears that the effect of the individual mutations at positions ^{384}R or ^{385}R with respect to the steady-state oxygen evolution rate is cumulative. The introduction of two negative charges at these sites (replacement of the two arginyl residues with glutamyl residues) produced a mutant (RR384385EE) with a more drastic impairment of evolution activity (40% of the control rate).

For comparison, the mutants Δ(A373−D380), Δ(R422−E428) (Haag et al., 1993), Δ(R384−V392) (Eaton−Rye & Vermaas, 1991), and Δ*psb*O (Burnap et al., 1991) have been included in Figure 1. The Δ(R422−E428) deletion mutant exhibits about 25% of the oxygen evolution capacity and accumulates about 15% of the PS II centers of the control strain. This mutant grows very slowly under photoautotrophic conditions (Haag et al., 1993). Interestingly, alteration of the conserved charged residues within this

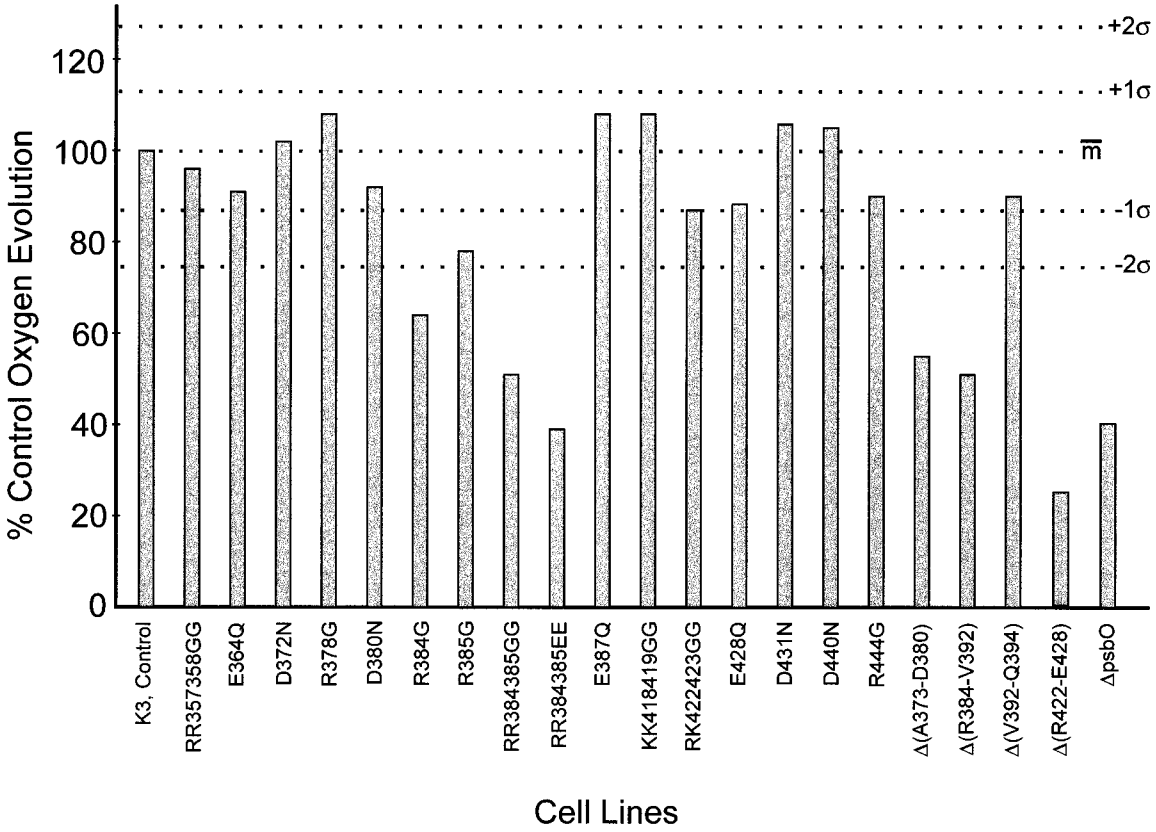

FIGURE 1: Oxygen evolution rates for the mutants described in this communication. These are the averages of three independent experiments. The control oxygen evolution rate for the K3 strain was 521 μmol of oxygen·(mg of Chl)$^{-1}$·h^{-1} with DCBQ as an electron acceptor. For comparison, the oxygen evolution rates for Δ(A373−D380), Δ(R384−V392), Δ(V392−Q394) (Haag et al., 1993), Δ(R384−V392) (Eaton-Rye & Vermaas, 1992), and Δ*psb*O (Burnap & Sherman, 1991), compared to their respective control strains, are shown. 1.0 and 2.0 standard deviation error envelopes about the control strain K3 are also shown.

deletion had little effect on either PS II activity or photoautotrophic growth. RK422423GG exhibits 87% the oxygen evolution activity of our control strain K3, while E428Q exhibits 100% of the control activity. Both of these mutants grew at rates comparable to that observed for the control strain (data not shown). This result demonstrates that the conserved charged residues removed in the Δ(R422−E428) deletion are not required for either normal rates of oxygen evolution (and by extension for PS II assembly/stability) or for photoautotrophic growth. The severe phenotype of Δ(R422−E428) is likely due to (1), the combined effect of the removal of ^{422}R, ^{423}K, and ^{428}E; (2) the removal of the conserved uncharged residues ^{425}Q and/or ^{427}G; or (3) is the result of a perturbation in the structure of CP 47 caused by deletion of seven residues. It should be noted that we have also modified all of the conserved charged residues which lie within most of the other severely affected deletion strains reported by Eaton-Rye and Vermaas (1991) and Haag et al. (1993). In all instances no significant decrease in oxygen evolution capacity or photoautotrophic growth rate was observed (C. Putnam-Evans and T. M. Bricker, in preparation). These results indicate that for the majority of the severely affected deletion strains which have been examined, hypothesis 3 is supported.

The deletions Δ(A373−D380) (Haag et al., 1993; Gleiter et al., 1994) and Δ(R384−V392) (Eaton-Rye & Vermaas, 1991) have phenotypes which are similar, but not identical, to that observed in the Δ*psb*O strain which lacks the 33 kDa extrinsic protein of PS II (Burnap & Sherman, 1991; Burnap et al., 1992). The steady-state oxygen evolution activityof the two deletion strains were about 50% of wild-type. The Δ*psb*O mutant evolves oxygen at about 40% of wild-type. Alteration of the conserved charged residues within Δ(A373−D380) yielded the mutants R378G and D380N, which exhibited oxygen evolution rates of 108% and 92%, respectively. As was the case for Δ(R422−E428) the diminution of the oxygen evolution rate in Δ(A373−D380) must be due to factors other than the loss of the conserved charged residues within the deletion domain. The loss of oxygen evolution activity observed in Δ(R384−V392) is very similar to that observed in the RR384385GG and RR384385EE mutants. Alteration of the final conserved charged residue within this deletion yielded the mutant E387Q, which exhibited no loss in oxygen evolution activity. These results suggest that, at least with respect to oxygen evolution activity, the phenotype of Δ(R384−V392) can be accounted for entirely by alterations at positions ^{384}R and ^{385}R.

Figure 2 shows the results of growth experiments performed with the mutants R384G, R385G, RR384385EE, and RR384385GG (Putnam-Evans & Bricker, 1992) as well as the control strain K3. All mutant strains were capable of supporting photoautotrophic growth. R384G and R385G grew at rates that were not significantly different from the control strain K3 and the mutation RR384385GG. RR384385EE, however, exhibited a decreased growth rate that was about 55% of that observed for the control strain K3. It is possible that this decreased growth rate is a product of the extreme susceptibility of this mutant to photoinactivation (see below), even at the low light intensities required

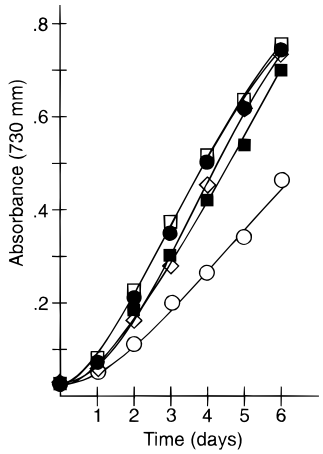

FIGURE 2: Photoautotrophic growth rates of the control strain K3 and mutants at positions ^{384,385}RR: closed square, K3; closed circle, R384G; open square, R385G; open diamond, RR384385GG; open circle, RR384385EE. These are the average of three independent experiments. Standard errors for these data averaged 3%−5% at each data point.

for cell growth. A similar phenomenon has been described in ^{190}H mutants in the D1 protein of *Chlamydomonas reinhardtii* (Roffey et al., 1994). None of the other mutant strains examined exhibited growth rates significantly different from the control strain K3 (data not shown). It is interesting to compare these results with growth experiments performed on the deletion strains Δ(A373−D380) (Haag et al., 1993), Δ(R384−V392) (Eaton-Rye & Vermaas, 1991) and Δ*psb*O (Burnap et al., 1992). Δ(A373−D380) and Δ(R384−V392) exhibit photoautotrophic growth characteristics which are very similar to their control strain. Δ*psb*O, however, exhibits a depressed growth rate that is about 65% of its control strain, which is comparable to that observed for RR384385EE.

Relative quantum yield experiments examining oxygen evolution rates were obtained at rate-limiting light intensities ranging from 25 to 150 μmol of photons$\cdot$m$^{-2}\cdot$s^{-1} (Table 2). At these low light intensities, examination of the first-order rate constants allows the estimation of the relative quantum yield exhibited by the control and mutant strains on a per chlorophyll basis. The relative quantum yields for R384G, R385G, RR384385GG, and RR384385EE were 0.59, 0.70, 0.64, and 0.40, respectively.

There are several ways to explain a decrease in the relative quantum yield: (1) The mutants may have, on a Chl basis, fewer PS II centers than does the control strain K3. The PS II centers which are present, however, could be normal with respect to oxygen evolution. (2) The mutants may have the same number of PS II centers as K3, but significant proportions of these PS II centers are inactive with respect to oxygen evolution. Again, those PS II centers which are active could be normal with respect to oxygen evolution. (3) The lower quantum yield could be the result of the presence of PS II centers which are less efficient in carrying out oxygen evolution. If, for instance, the introduction of a site-directed mutation at these sites leads to a decrease in the ability of the oxygen-evolving complex to reduce Y_Z^+, a lowered oxygen evolution rate would be observed. PS II centers which are less efficient at coupling quantum absorption with advancement of the water-oxidizing complex would be expected to exhibit a higher miss probability in flash oxygen yield measurements. However, this was not observed (see below), leading us to conclude that the reduced quantum yield is due to either a lower concentration of reaction centers or a normal concentration of reaction centers but with a large fraction of these centers incapable of oxygen evolution.

To estimate the concentration of PS II reaction centers in these mutants (Table 2) we measured the variable fluorescence yield. Analysis of the variable fluorescence yield gives a semiquantitative estimate of the relative concentration of PS II centers (Nixon & Diner, 1992; Chu et al., 1994). The variable fluorescence yields for R384G, R385G, RR384385GG, and RR384385EE were 0.85, 0.91, 0.84, and 0.85, respectively, indicating that these mutants contain only a slightly lower number of total PS II centers than the control strain K3. Since the relative quantum yield measurements indicate that a lower number of oxygen-evolving centers per chlorophyll are present in these mutants, these fluorescence results suggest that mutations introduced at positions ^{384,385}RR results in a substantial decrease in the fraction of PS II centers capable of evolving oxygen. Thus, the mutants appear to assemble near-normal levels of PS II reaction centers but a significant fraction of these does not evolve oxygen. These results must be interpreted with caution, because other parameters, such as a lower excitation energy transfer efficiency or an alteration of the rate constant of charge separation and its dependence on the redox state of Q_A, could theoretically affect the fluorescence yield. It should be noted, however, that the combined analysis of 21 D1 mutants (Chu et al., 1994) and eight deletion mutants in the large extrinsic loop of CP 47 (Gleiter et al., 1994) indicates that there is a strong correlation ($r = 0.9$) between the relative concentration of PS II centers as determined either by [^{14}C]DCMU-binding or by total fluorescence yield (analysis not shown).

We found that the PS II centers capable of oxygen evolution in these mutants were more sensitive to photoinactivation than PS II centers in the control strain K3 (Table 2). At 4000 μmol of photons$\cdot$m$^{-2}\cdot$s^{-1}, the mutants R384G and R385G photoinactivated approximately twice as fast as the control. The double mutant RR384385EE was even more susceptible to this photoinactivation treatment, exhibiting a 4-fold increase in the rate of photoinactivation. Previously, we had shown that the mutant RR384385GG photinactivated twice as fast as the control strain (Putnam-Evans & Bricker, 1992).

The increased susceptibility of R384G, R385G, and RR384385GG to photoinactivation was comparable in magnitude to that observed in the E69Q and P161L mutants in the D2 protein (van der Bolt & Vermaas, 1992) and the R448G mutant in CP 47 of *Synechocystis* (Putnam-Evans & Bricker, 1994), while the RR384385EE mutant exhibited a more extreme sensitivity. The E69Q mutation is believed to affect the stability and/or ligation of the manganese cluster while the P161L mutation is located near Y_D and is believed to affect the efficiency of transfer of electrons from the oxygen-evolving site to Y_Z^+ (van der Bolt & Vermaas, 1992). The R448G mutant in CP 47 may alter a chloride-binding site in PS II (Putnam-Evans & Bricker, 1994). These authors hypothesized that decreased rates of electron transfer from the oxygen-evolving complex to Y_Z^+, which was observed in these mutants, resulted in the accumulation of oxidizing-side radicals (such as Y_Z^+ and P680$^+$) which damage the PS II reaction center and lead to the observed photoinactivation. It appears that a similar mechanism may be occurring in the mutants which we have examined in this communica-

Table 2: Photosynthetic Parameters of the Control and Mutant Strains

cell type	oxygen evolution rate[a,b,c]	quantum yield for oxygen evolution[a,b,c]	$(F_v/F_0)_{mutant}$ [b,c,d] / $(F_v/F_0)_{control}$	photoinactivation $(T_{1/2,control}/T_{1/2,mutant})$[a,e]
control	521± 22	1.00 ± 0.04	1.00 ± 0.07	1.0
R384G	334 ± 17	0.59 ± 0.02	0.85 ± 0.09	2.1
R385G	405 ± 32	0.70 ± 0.15	0.91 ± 0.02	2.0
RR384385GG	271 ± 28	0.64 ± 0.05 [f]	0.84 ± 0.08	2.0[d]
RR384385EE	204 ± 12	0.40 ± 0.05	0.85 ± 0.04	4.0

[a] Electron transport from water to DCBQ. [b] Data are from at least three independent experiments. [c] ±1.0 standard error is indicated. [d] The F_v/F_o for the control strain was 0.66 ± 0.05. [e] Data from two independent experiments. The control $T_{1/2}$ was 8.5 min. [f] Data from Putnam-Evans and Bricker (1992).

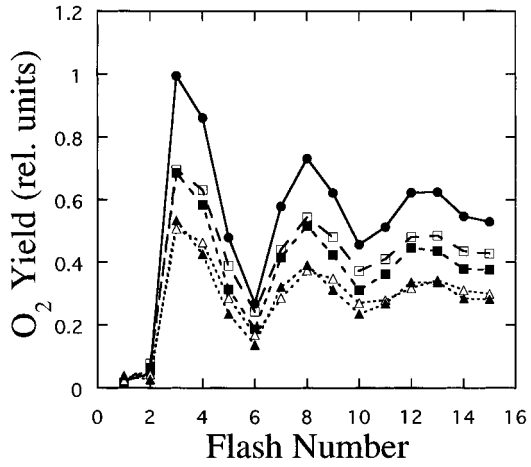

FIGURE 3: Amplitudes of oxygen yield as a function of flash number. Cells were centrifugally deposited on a bare platinum electrode, dark adapted for 10 min, and given a train of saturating, single-turnover xenon flashes at 3 Hz frequency. Closed circles, K3; open squares, R384G; closed squares, R385G; open triangles, RR384385GG; closed triangles, RR384385EE.

tion. Examination of the rate of release of oxygen from the PS II reaction centers of these mutants supports this hypothesis (see below).

The patterns of oxygen yield by the dark-adapted mutant and the control strain K3 cells were measured on a bare platinum electrode under a sequence of saturating, single-turnover flashes given at a frequency of 3 Hz. Figure 3 depicts the amplitude of the oxygen yield as a function of flash number. The amplitudes of the oxygen signals in the mutants were decreased in comparison to K3, with the double substitution mutants being the most severely depressed. The reduced amplitudes of the mutants are consistent with the relative quantum yield experiments and the steady-state oxygen evolution rates described above. Despite the reduced amplitudes, all of the mutants exhibited the characteristic period four oscillations in oxygen yield, indicating that the basic mechanism of water oxidation remains largely unchanged in the mutant reaction centers. To evaluate possible alterations in the transition probabilities associated with the four-step water oxidation mechanism, the oscillatory patterns were analyzed using an eigenvector method to estimate the parameters α, β, γ, and δ, which correspond to misses, hits, double hits, and deactivations, respectively (Meunier, 1993). These results are summarized in Table 3. Only relatively moderate increases in the miss probability α in the double substitution mutants were detected with this analysis. The larger average miss probabilities estimated for the double-substitution mutants suggest that positive charges generated in the mutant reaction centers are less efficiently utilized for the advancement of the water oxidizing complex through the sequence of S-states leading to oxygen evolution. However, this modest increase in the miss probability suggests that it alone cannot account for the reduction in apparent flash oxygen yield and the quantum yields observed in the mutants. These results are consistent with an analysis of Δ(A373−D380) which also exhibited relatively little change in the oscillatory patterns of flash oxygen yield (Gleiter et al., 1994).

Although the oscillatory patterns of oxygen flash yield were not significantly altered in these mutants, there were large changes in the kinetic properties for oxygen evolution. Kinetically resolved oxygen signals of the mutant and K3 cells are shown in Figure 4. The rise of the signals for the mutants was consistently slower than that seen for the control strain measured under identical conditions. An empirical approach to the kinetic analysis of oxygen signals, assuming single exponentials for their rise and decay, was previously found to provide a reasonable fit to the shape of the oxygen signal (Jursinic & Dennenberg, 1990; Burnap et al., 1992). Using a modification of this approach (Figure 3, legend), we have quantified the exponential rise kinetic, τ_r, of the oxygen pulse for each of the mutants examined in Table 3. The τ_r for the K3 control sample was found to be 3 ms, which is generally in accordance with previous findings with control samples analyzed in a similar manner (Jursinic & Dennenberg, 1990; Meunier & Popovic, 1991; Burnap et al., 1992; Lavorel, 1992). The mutant signals were found to be markedly slower, with the RR384385EE mutant exhibiting a release time of nearly 8 ms. The rise time of the oxygen signal depends upon the rate constant for oxygen release by the oxygen-evolving complex and the diffusion time of oxygen out of the cell and through the intervening buffer to the electrode surface. The actual rate of oxygen release by the native oxygen-evolving complex is presumed to be on the order of 1−2 ms (Joliot et al., 1966; Etienne, 1968; Babcock et al., 1976; Meunier & Popovic, 1991). The electrode we used cannot kinetically resolve this process. The τ_r of the K3 signal is about 3 ms, which appears to be dominated by the diffusion time required for oxygen to reach the electrode surface. Since the mutant strains and K3 were treated identically it is not expected that the parameters governing diffusion are different between the samples. The slower rise time of the oxygen signal in the flashed mutant cells is assumed to indicate slower oxygen release kinetics. This may reflect an alteration in the oxygen-yielding $S_3-[S_4]-S_0$ transition in the mutants. The $S_3-[S_4]-S_0$ transition of wild type is approximately 1.2 ms (Bouges-Bocquet, 1973; R. Burnap et al., to be submitted). If the 7−8 ms rise of the oxygen signal in the mutants represents a truly kinetically resolvable $S_3-[S_4]-S_0$ transition (or oxygen release), then the mutations produce a 6−7-fold retardation in the kinetics

Table 3: Oxygen Yield Characteristics of the Control and Mutant Strains

strain	α, misses[a]	β, single-hits[a]	γ, double-hits[a]	δ, deactivations	τ_r, risetime of oxygen signal (ms)[a,b]	S_2 half-life (s)[c]
K3	15	83	1	1	3	18
R384G	16	81	2	1	7	37
R385G	16	82	1	1	7	35
RR384385GG	18	79	1	2	8	33
RR384385EE	19	79	1	1	8	55

[a] Estimated by analysis of the oscillation of flash oxygen yield amplitudes on the bare platinum electrode using the eigenvector analysis method of Meunier (1993). [b] Obtained from the kinetic analysis of oxygen transients as described in Figure 4. [c] Measured by following the decay of the amplitude of the oxygen yield on the third flash as a function of increasing the time interval between the first and second flashes (Forbush et al., 1971).

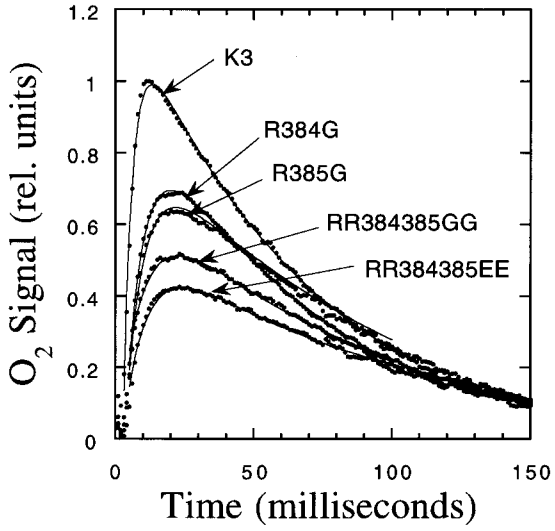

FIGURE 4: Oxygen signals of cells on a bare platinum electrode illuminated with a saturating xenon flash. Cells were given 30 flashes prior to acquisition of the signals shown in order to achieve mixing of the S-state distribution of the PS II centers in the samples. The actinic flash occurred at time zero on the ordinate for each sample and the signals were recorded digitally at a rate of 1 data point per millisecond. Data points are depicted as dots. Solid lines represent fits to the equation $f(t) = (1 - ae^{-k_r t}) + be^{-k_d t}$, where k_r and k_d represent the rise and decay of the signal, respectively, and *a* and *b* represent scaling factors. The exponential rise times of the oxygen signals depicted in this figure are shown in Table 3.

of oxygen production. The slower release time may significantly affect the V_{max} of oxygen evolution with DCBQ as the acceptor because the 7−8 ms mutant S-state transition time is greater in magnitude than the acceptor side turnover limitation with optimal DCBQ concentrations [about 5 ms; M. Qian and R. Burnap, unpublished observations; also see Myers & Graham (1983) and Lee and Whitmarsh, (1989)]. A retarded $S_3-[S_4]-S_0$ transition may increase the probability of photoinactivation due to the comparatively long-lived nature of the potentially destructive oxidizing equivalent on the donor side of the reaction center therby explaining the increased tendency toward photoinactivation exhibited by these mutants.

Measurements of the lifetime of the S_2 state for the control and mutant strains were made by recording the amplitude of the oxygen signal on the third flashes as a function of increasing the time interval between the first and second flash (Table 3) (Forbush et al., 1971; Nixon & Diner, 1992). The mutants R384G, R385G, and R384385GG exhibited S_2 lifetimes that were about twice as long as that observed in the control strain. The mutant RR384385EE exhibited a lifetime that was three times longer than that of the control. These results indicate that alteration of the charge density at positions 384 and 385 in CP 47 leads to an increased apparent stability of the S_2 state. The decay of the S_2 state corresponds to a charge recombination process involving an oxidizing equivalent in the water-oxidizing complex and a reductant, possibly Q_A^-, Q_B^-, or some other exogenous reductant. Alterations in the rate of charge recombination can, in principal, reflect changes in the redox properties of either the oxidized or reduced species of the charge pair. Major changes in the redox properties of the acceptor side in these mutants can probably be ruled out since the more radical deletion mutations encompassing ^{384,385}RR do not exhibit altered reoxidation kinetics of Q_A^- by Q_B (or Q_B^-) (Gleiter et al., 1994, 1995). Their results indicate that the acceptor side remains relatively intact even in the more disrupted deletion strains. This suggests that changes in the dark stability of the S_2 state may reflect changes in the redox properties of the manganese cluster. In the context of the results of Gleiter et al. (1994, 1995) the basic residue pair mutants appear to most closely resemble the Δ(A373−D380) and Δ(R384−V392) mutants with respect to decay of the S_2 state. Although direct comparison of the decay times are problematic due to differences in the experimental conditions, the relative increase in the decay times relative to the respective control strains is 1.5−3-fold in both cases. However, the extent to which these mutations also affect the redox properties of Y_Z, P_{680}, and the acceptor side components of PS II remains to be established, and, therefore, changes to the lifetime of the S_2 state due to alterations in the redox properties of these species cannot be excluded.

The structural basis for the observed phenotypes of the mutants which we have examined is unclear. Alteration of these arginyl residues in this region of CP 47 could lead to global structural perturbations within CP 47 and/or other PS II components. Alternatively, these positively charged residues may serve as protein−protein interaction sites either within CP 47 or between CP 47 and another PS II component(s). This ambiguity exists for virtually all site-directed mutations which have been produced in PS II. An obvious candidate for such a hypothetical interaction is the 33 kDa extrinsic protein of PS II. Numerous lines of evidence show a close interaction between CP 47 and the extrinsic 33 kDa protein (Bricker & Frankel, 1987; Enami et al., 1987; Frankel & Bricker, 1989, 1992), and these proteins have been demonstrated to associate via a charge-pair interaction (Bricker et al., 1988; Enami et al., 1991; Odom & Bricker, 1992) with the domain ^{364}E−^{440}D of CP 47 being cross-linked with the water-soluble carbodiimide EDC to the domain ^{2}E−^{76}K of the 33 kDa protein.

Comparison of Δ*psb*O strains, which lack the 33 kDa extrinsic protein (Burnap & Sherman; 1991), the CP 47

partial deletion strains, Δ(R384−V392) and Δ(A373−D380) (Eaton-Rye & Vermaas, 1991; Haag et al., 1993), and the site-directed mutants (particularly RR384385GG and RR384385EE) which we have examined yield several similarities as well as some intriguing differences. All of these strains exhibit similar rates of steady-state oxygen evolution, have increased rates of photoinactivation, and exhibit longer S_2-state lifetimes. Our mutants and the Δ*psb*O strain possess an apparently retarded $S_3-[S_4]-S_0$ transition, a parameter which has not been measured in the partial deletion strains. Gleiter et al. (1994) have reported that Δ(R384−V392) and Δ(A373−D380) bind the extrinsic 33 kDa protein with lower affinity than their control strain. We have observed that PS II particles prepared from RR384385GG entirely lack the extrinsic 33 kDa extrinsic protein (C. Putnam-Evans and T. M. Bricker, unpublished observations). Attempts to duplicate the methodology utilized by Gleiter et al. (1994), however, yielded erratic results with all of the mutants described in this communication. This may suggest that the phenotype of the partial deletion strains is more extreme with respect to 33 kDa extrinsic protein binding.

It is noteworthy that the Δ(R384−V392), Δ(A373−D380), and Δ*psb*O strains all exhibit rapid dark inactivation ($T_{1/2}$ = minutes). Also, the rate of photoactivation (after dark inactivation) of Δ(R384−V392) and Δ(A373−D380) is markedly accelerated by the addition of high concentrations of calcium (Gleiter et al., 1995). An earlier study showed that Δ*psb*O strains did not exhibit photoautotrophic growth at low calcium concentrations (Philbrick et al., 1991). Thus, the partial deletion strains and the Δ*psb*O mutant exhibit rather significant calcium effects. The site-directed mutants which we have examined exhibit extremly slow dark photoinactivation ($T_{1/2}$ = 10 h; R. Burnap, unpublished observations) and exhibit normal photoautotrophic growth in calcium deficient media (C. Putnam-Evans and T. M. Bricker, unpublished observations). We speculate that in the partial deletion strains and the Δ*psb*O mutant the normal association of calcium with the PS II reaction center is disrupted. This leads to a decreased stability of the oxygen-evolving complex and results in rapid dark inactivation. The site-directed mutants which we have examined at positions ^{384,385}RR appear to possess a relatively normal calcium−PS II interaction. This suggests that the phenomena of rapid dark inactivation (and associated calcium effects) are not *per se* directly associated with the phenotypes observed in all of the mutants which are directly attributable to a defective oxygen-evolving apparatus (i.e., decreased oxygen evolution rate, increased photoinactivation, increased S_2 lifetime, and $S_3-[S_4]-S_0$ transition retardation).

REFERENCES

Babcock, G. T., Blankenship, R. E., & Sauer, K. (1976) *FEBS Lett. 61*, 286−289.

Bouges-Bocquet, B. (1973) *Biochim. Biophys. Acta. 292*, 772−785.

Bricker, T. M. (1990) *Photosynth. Res. 24*, 1−13.

Bricker, T. M. (1992) *Biochemistry 31*, 4623−4628.

Bricker, T. M., & Frankel, L. K. (1987) *Arch. Biochem. Biophys. 256*, 295−301.

Bricker, T. M., Odom, W. R., & Queirolo, C. B. (1988) *FEBS Lett. 231*, 111−117.

Burnap, R. L., & Sherman, L. A. (1991) *Biochemistry 3*0, 440−446.

Burnap, R., Shen, J. R., Jursinic, P. A., Inoue, Y., & Sherman, L. A. (1992) *Biochemistry 31*, 7404−7410.

Chu, H.-A., Nguyen, A. P., & Debus, R. J. (1994) *Biochemistry 33*, 6137−6149.

Debus, R. J. (1992) *Biochim. Biophys. Acta 1102*, 269−352.

Eaton-Rye, J. J., & Vermaas, W. F. J. (1991) *Plant Mol. Biol. 17*, 1165−1177.

Enami, I., Satoh, K., & Katoh, S. (1987) *FEBS Lett. 226*, 161−165.

Enami, I., Kaneko, M., Kitamura, N., Koike, H., Sinoike, K., Inoue, Y., and Katoh, S. (1991) *Biochim. Biophys. Acta 1060*, 224−232.

Etienne, A. L. (1968) *Biochim. Biophys. Acta 153*, 895−897.

Forbush, B., Kok, B., & McGloin, M. P. (1971) *Photochem. Photobiol. 14*, 307−321.

Frankel, L. K., & Bricker, T. M. (1989) *FEBS Lett. 257*, 279−282.

Frankel, L. K., & Bricker, T. M. (1990) in *Current Research in Photosynthesis* (Batcheffsky, M., Ed.), Vol. 1, pp 825−828, Kluwer Academic Press, Dordrecht, The Netherlands.

Frankel, L. K., & Bricker, T. M. (1992) *Biochemistry 31*, 11059−11064.

Gleiter, H. M., Haag, E., Shen, J.-R., Eaton-Rye, J. J., Inoue, Y., Vermaas, W. F. J., & Renger, G. (1994) *Biochemistry 33*, 12063−12071.

Gleiter, H. M., Haag, E., Shen, J.-R., Eaton-Rye, J. J., Seeliger, A. G., Inoue, Y., Vermaas, W. F. J., & Renger, G. (1995) *Biochemistry 34*, 12063−12071.

Haag, E., Eaton-Rye, J. J., Renger, G., & Vermaas, W. F. J. (1993) *Biochemistry 32*, 4444−4454.

Hayashi, H., Fujimura, Y., Mohanty, P. S., & Murata, N. (1993) *Photosynth. Res. 36*, 35−42.

Joliot, P., Hofnung, M., & Chaubaud, R. (1966) *J. Chem. Phys. 63*, 1423−1441.

Jursinic, P. A., & Dennenberg, R. J. (1990) *Biochim. Biophys. Acta* 1020, 195−206.

Kunkel, T. A. (1985) *Proc. Natl. Acad. Sci. U.S.A. 82*, 488−492.

Lavorel, J. (1992) *Biochim. Biophys. Acta 1101*, 33−40.

Lee, W. J., & Whitmarsh, J. (1989) *Plant Physiol. 89*, 932−940.

Meunier, P. C. (1993) *Photosynth. Res. 36*, 111−118.

Meunier, P. C., & Popovic, R. (1991) *Photosyn. Res. 28*, 33−39.

Maniatis, T., Fritsch, E. F., & Sambrook, J. (1982) *Molecular Cloning:* A *Laboratory Manual*, Cold Spring Harbor Laboratory, Cold Spring Harbor Laboratory Press, Plainview, NY.

Myers, J., & Graham, J. R. (1991) *Biochim. Biophys. Acta 722*, 281−290.

Nixon, P., & Diner, B. (1992) *Biochemistry 31*, 942−948.

Odom, W. R., & Bricker, T. M. (1992) *Biochemistry 31*, 5616−5620.

Philbrick, J. B., Diner, B. A., & Zilinskas, B. A. (1991) *J. Biol. Chem. 266*, 13370−13376.

Putnam-Evans, C., & Bricker, T. M. (1992) *Biochemistry 31*, 11482−11488.

Putnam-Evans, C., & Bricker, T. M. (1994) *Biochemistry 33*, 10770−10776.

Rippka, R., Derulles, J., Waterbury, J. B., Herdman, M., & Stanier, R. Y. (1979) J. *Gen. Microbiol. 111*, 1−61.

Roffey, R. A., van Wijk, K. J., Sayre, R. T., & Styring, S. (1994) *J. Biol. Chem. 269*, 5115−5121.

van der Bolt, F., & Vermaas, W. (1992) *Biochim. Biophys. Acta 1098*, 247−254.

Vermaas, W. F. J., Williams, J. G. K., & Arntzen, C. J. (1987) *Plant Mol. Biol. 8*, 317−326.

Vermaas, W. F. J., Ikeuchi, M., & Inoue, Y. (1988) *Photosyn. Res. 17*, 97−113.

Williams, J. G. K. (1988) *Methods Enzymol. 167*, 766−778.

BI952661S